

Alternating cyclic extrapolation methods for optimization algorithms

Nicolas Lepage-Saucier*

August 2021

Abstract

This article introduces new acceleration methods for fixed-point iterations. Extrapolations are computed using two or three mappings alternately and a new type of step length is proposed with good properties for nonlinear applications. The methods require no problem-specific adaptation and are especially efficient in high-dimensional contexts. Their computation uses few objective function evaluations, no matrix inversion and little extra memory. A convergence analysis is followed by eight applications including gradient descent acceleration for constrained and unconstrained optimization. Performances are on par with or better than competitive alternatives. The algorithm is available as the Julia package `SpeedMapping.jl`.

Keywords: fixed point; mapping; extrapolation; nonlinear optimization; acceleration technique; vector sequences; gradient descent; quasi-Newton

1 Introduction

Let $F : \mathbb{R}^n \rightarrow \mathbb{R}^n$ denote a mapping which admits continuous, bounded partial derivatives. Finding a fixed point of F , $x^* : F(x^*) = x^*$, is the basis of countless numerical applications in disciplines like statistics, computer science, physics, biology, and economics, driving the development of many general and domain-specific iterative methods. For reviews and insightful comparisons of the most important ones, see notably Jbilou and Sadok (2000), Ramière and Helfer (2015), Brezinski et al. (2018) and the textbook by Brezinski and Redivo-Zaglia (2020).

One of these methods is a vector version of Aitken's Δ^2 process usually attributed to Lemaréchal (1971) but also discovered by Irons and Tuck (1969) and Jennings (1971). Following Aitken's notation, define $\Delta x = F(x) - x$ and note that at the fixed point of

*Concordia University Corresponding address: nicolas.lepagesaucier@concordia.ca

F , $\Delta x^* = \mathbf{0}$. Lemaréchal's method may be interpreted as a simplified quasi-Newton method for finding a root of Δx :

$$x_{k+1} = x_k - M_k^{-1} \Delta x_k \quad (1)$$

where M_k is the approximation of the Jacobian of Δx_k . It takes the simple form $M_k = s_k^{-1} I$, where s_k is a scalar and, contrary to other quasi-Newton methods, it ignores off-diagonal elements. The Jacobian is approximated by the secant method using two consecutive evaluations of the mapping F :

$$\frac{d\Delta x_k}{dx_k} \approx \frac{\Delta^2 x_k}{\Delta x_k}.$$

where $\Delta^2 x_k = \Delta F(x_k) - \Delta x_k = F(F(x_k)) - 2F(x_k) + x_k$, and, in general, $\Delta^p x = \Delta^{p-1} F(x) - \Delta^{p-1} x$ for $p \in \mathbb{N}^+$. The step length is

$$s_k = \arg \min_s \left\| s^{-1} I - \frac{\Delta^2 x_k}{\Delta x_k} \right\|^2 = \frac{\langle \Delta^2 x_k, \Delta x_k \rangle}{\|\Delta^2 x_k\|^2} \quad (2)$$

where $\|y\|_p$ is the p -norm of a vector y , $\|y\| = \|y\|_2 = \sqrt{y^\top y}$ is the 2-norm of a vector y , and $\langle y, z \rangle = y^\top z$ is the inner product of vectors y and z . Substituting s_k in (1), an iteration of Lemaréchal's method is

$$x_{k+1} = x_k - \frac{\langle \Delta^2 x_k, \Delta x_k \rangle}{\|\Delta^2 x_k\|^2} \Delta x_k. \quad (3)$$

Early on, this simple way of computing the step length proved to be generally faster and more stable than comparable techniques (see Henrici (1964) or Macleod (1986)). It was later improved upon by Barzilai and Borwein (1988). The Barzilai-Borwein (BB) method requires a single mapping per iteration by using the Cauchy step length of the previous iteration. It spawned a rich line of research in gradient-based optimization for linear problems, a branch of which investigates the link between the optimal step size and the Hessian spectral properties (see Birgin et al. (2014) for a good review), to which this paper is also relevant.

As will be argued, this choice of s_k may cause slow convergence if the Jacobian of Δx has a wide spectrum. To avoid this drawback, new step lengths will be introduced to target specific deviations of x from its fixed point and considerably speed-up convergence over time.

For exposition, let us consider a system of linear equations

$$Ax = b$$

where $A \in \mathbb{R}^{n \times n}$ and $b \in \mathbb{R}^n$. The solution of the system also constitutes the minimizer of the quadratic function $f(x) = \frac{1}{2} x^\top A x - x^\top b$ with gradient $\nabla f(x) = Ax - b$ and Hessian A . To avoid the need for a change of coordinates, assume $A = \text{diag}(\lambda_1 \dots \lambda_n)$

with positive entries and $m \leq n$ distinct eigenvalues with the smallest and largest labeled λ_{\min} and λ_{\max} , respectively.

The problem may be formulated as finding the fixed point to the mapping

$$F(x) = x - (Ax - b),$$

with unique solution x^* representing a fixed point of F at which $Ax^* = b$. To study the convergence of the method, define an error as $e = x - x^*$. Direct computation gives $\Delta x = -(Ax - b) = -Ae$ and, in general, $\Delta^p x = (-A)^p e$. Since A is diagonal, s_k may be expressed as

$$s_k = \frac{\langle A^2 e_k, -Ae_k \rangle}{\|A^2 e_k\|^2} = -\frac{e_k^\top A^3 e_k}{e_k^\top A^4 e_k} = -\frac{\sum_{i=1}^n \left(e_k^{(i)} \lambda_i^2 \right)^2 \frac{1}{\lambda_i}}{\sum_{i=1}^n \left(e_k^{(i)} \lambda_i^2 \right)^2}. \quad (4)$$

We can write (3) in terms of errors and obtain for the linear system

$$e_{k+1} = (I + s_k A) e_k.$$

In particular, the j^{th} error component may be individually expressed as

$$e_{k+1}^{(j)} = (1 + s_k \lambda_j) e_k^{(j)}, \quad j = 1, \dots, n. \quad (5)$$

As shown by (5), if s_k was somehow set exactly equal to $-\frac{1}{\lambda_j}$, the error $e_{k+1}^{(j)}$ would be perfectly annihilated. It would also remain zero for all subsequent iterations, regardless of s_{k+1}, s_{k+2}, \dots . Since A has m distinct eigenvalues, all error components could be successively reduced to zero in m iterations. Conversely, from a starting point with at least one positive error component $e_0^{(j)}$ for each distinct eigenvalue, m is also the minimum number of steps necessary to annihilate all $e^{(j)}$ exactly. Of course, as shown by (4), $s_k \in [-\lambda_{\min}^{-1}, -\lambda_{\max}^{-1}]$ is a weighted average of all negative inverse eigenvalues. As a result, all $e^{(j)}$ are imperfectly reduced simultaneously at each iteration and convergence may be slow if A has a wide spectrum.

Instead, targeting specific error components may be more efficient. To do so, note that at the fixed point x^* , any higher-order difference $\Delta^p x$ is zero, not only Δx . The rate of change of $\Delta^p x$ for $p > 1$ also carries useful information on the location of the fixed point. Define a step length of order p as

$$s^{(p)} = \frac{\langle \Delta^p x, \Delta^{p-1} x \rangle}{\|\Delta^p x\|^2} \quad (6)$$

where $s^{(2)} \equiv s$ defined in (2) is a special case. In particular, a ‘‘cubic’’ step length $s^{(3)}$ may be interpreted as the change in $\Delta^3 x$ following a change of $\Delta^2 x$. In the linear example, $s_k^{(3)}$ would be

$$s_k^{(3)} = -\frac{e_k^\top A^5 e_k}{e_k^\top A^6 e_k} = -\frac{\sum_{i=1}^n \left(e_k^{(i)} \lambda_i^3 \right)^2 \frac{1}{\lambda_i}}{\sum_{i=1}^n \left(e_k^{(i)} \lambda_i^3 \right)^2}.$$

Using $s_k^{(3)}$ for approximating the Jacobian of Δx_k puts more weights on eigenvalues of larger magnitudes and should annihilate the associated errors more aggressively. After such step k , a squared step $k + 1$ should target errors associated with smaller eigenvalues more precisely since the error associated with larger ones would have a lighter weight in $s_{k+1}^{(2)}$. The algorithm can then continue alternating between cubic and squared extrapolations.

Schemes based on squared iterations alone rely on the hope that Δx changes at similar rates for all components of e which is false if A has a wide spectrum. Starting with a cubic extrapolation selects a path in parameter space where the following squared extrapolation suffers less from this source of error. A single cubic iteration may not converge faster but alternating between different orders may dynamically enhance convergence over time.

Of course, computing higher-order step lengths requires more mappings.¹ Fortunately, this extra compute cost is mitigated by the ability to use $s^{(p)}$ for many extrapolations thanks to the important idea of cycling (Friedlander et al. (1999) and Raydan and Svaiter (2002)). Raydan and Svaiter noted that the iterates of the BB method are themselves mappings with the same fixed point x^* and that the same step length could be used for a second extrapolation with little extra computational cost. To understand the idea, denote an intermediate series $y_{k,(i)}$ constructed from Lemaréchal’s method applied to $x_k, F(x_k), F(F(x_k)), \dots$: $y_{k,(1)} = x_k - s_k \Delta x_k$, $y_{k,(2)} = F(x_k) - s_k \Delta F(x_k)$, \dots . Note that the series $y_{k,(1)}, y_{k,(2)}, \dots$ also converges to x^* and can therefore be extrapolated in the same fashion and using the same step length:

$$y_{k+1} = y_{k,(1)} + s_k(y_{k,(2)} - y_{k,(1)})$$

After substitution, the squared cyclic extrapolation can be written as

$$x_{k+1} = y_{k+1} = x_k - 2s_k \Delta x_k + s_k^2 \Delta^2 x_k.$$

This Cauchy-Barzilai-Borwein (CBB) method has good convergence properties. It was successfully adapted to a variety of nonlinear contexts by Varadhan and Roland (2004, 2005 and 2008), notably to accelerate the expectation maximization (EM) algorithm (Ortega and Rheinboldt (1970), Dempster et al. (1977)) under the label SQUAREM.

For a p -order step, cycling may be performed p times in the same recursive manner. In the linear system previously defined, with a step $s_k^{(p)}$ and p -order cycling, the error e_{k+1} becomes

$$e_{k+1} = \left(I + s_k^{(p)} A \right)^p e_k.$$

By cycling and alternating between different extrapolation orders, the proposed scheme is best understood as an alternating cyclic extrapolation method (ACX). Two specific schemes will be studied empirically: ACX^{3,2}, which alternates between cubic ($p = 3$) and

¹It may explain why few acceleration schemes requiring third-order or even higher-order differences have been put forth. Notable exceptions are Marder and Weitzner (1970), Lebedev and Zabelin (1995) and Brezinski and Chehab (1998).

squared ($p = 2$) extrapolations, and ACX^{3,3,2} which performs two cubic extrapolations before one squared extrapolation. They display good overall empirical properties, but higher order extrapolations or other sequences could be considered in specific contexts. For simplicity, ACX will be shorthand for any of these two methods in the rest of the paper.

The next section describes the algorithm formally and introduces a new type of step length with good properties for ACX in nonlinear contexts. Section 3 establishes Q-linear convergence of ACX for linear mappings in a suitable norm and discusses its convergence properties in nonlinear contexts. Section 4 discusses stability issues and implementation details, including an adaptation of ACX to gradient descent acceleration with dynamic adjustment of the descent step size.

ACX has many advantages. It can be used “as-is” for a wide variety of problems without extra specialization and close to no tuning. It requires few to no objective function evaluations, no matrix inversion, and little extra memory. It stands to shine in high dimensional applications which are ever more prevalent with the proliferation of large datasets and sparse data structures.

These advantages are on display in Section 5. ACX is applied to gradient descent acceleration for various constrained and unconstrained optimizations including 96 problems from the CUTEst collection (see Bongartz et al. (1995)). It compares favorably to popular methods like the limited-memory Broyden–Fletcher–Goldfarb–Shanno algorithm (L-BFGS) (see Liu and Nocedal (1989) and Nocedal and Wright (2006)) and the nonlinear conjugate gradient method (N-CG) proposed by Hager and Zhang (2006). It also performs well for various other fixed-point iterations compared to competitive alternatives like the quasi-Newton acceleration of Zhou et al. (2011), the objective acceleration approach of Riseth (2019), the Anderson acceleration version of Henderson and Varadhan (2019), and other domain-specific algorithms.

ACX is available as the Julia package SpeedMapping.jl.

2 Alternating-orders cyclic extrapolations

A p -order ACX iteration may be synthesized as:

$$x_{k+1} = \sum_{i=0}^p \binom{p}{i} (\sigma_k^{(p)})^i \Delta^i x_k \quad p \geq 2 \quad (7)$$

where $\Delta^0 x_k = x_k$, $\binom{p}{i} = \frac{p!}{i!(p-i)!}$ is a binomial coefficient, and $\sigma_k^{(p)} = |s_k^{(p)}| \geq 0$ is the absolute value of the step length (6).

Step lengths other than s (2) (sometimes referred to as s^{BB2}), have been suggested in the literature. Barzilai and Borwein (1988) suggested $s^{BB1} = \|\Delta x\|^2 / \langle \Delta^2 x, \Delta x \rangle$. Roland and Varadhan (2008) introduced $s^{RV} = -\sqrt{s^{BB1} s^{BB2}} = -\|\Delta x\| / \|\Delta^2 x\|$ (this author’s notation), commenting that for nonlinear mappings, s^{BB1} can compromise stability since the denominator $\langle \Delta^2 x, \Delta x \rangle$ may be close to zero or even positive. Similarly,

s^{BB2} may be problematic if $\langle \Delta^2 x, \Delta x \rangle$ is positive and $\|\Delta^2 x\|^2$ is small. In contrast, s^{RV} has a guaranteed negative sign for better overall stability. In the case of ACX^{3,2} and ACX^{3,3,2} however, an even better choice turns out to be $-\sigma^{(p)} \equiv -|s^{(p)}|$. It is a simple way of avoiding wrong signs while providing better overall convergence. Other options could be explored given the growing literature on optimal step sizes for descent algorithms (see for instance Dai et al. (2019) for a recent contribution).

The ACX algorithm is formalized as follows.

Algorithm 1 *Input: a mapping $F : \mathbb{R}^n \rightarrow \mathbb{R}^n$, a starting point $x_0 \in \mathbb{R}^n$, and a vector of orders (o_1, \dots, o_P) with $o_j \in \{2, 3\}$.*

```

1   for  $k = 0, 1, 2, \dots$  until convergence
2        $p_k = o_{(k \bmod P)+1}$ 
3        $\Delta^0 = x_k$ 
4        $\Delta^1 = F(x_k) - x_k$ 
5        $\Delta^2 = F^2(x_k) - 2F(x_k) + x_k$ 
6       If  $p_k = 3$ :  $\Delta^3 = F^3(x_k) - 3F^2(x_k) + 3F(x_k) - x_k$ 
7        $\sigma_k^{(p_k)} = |\langle \Delta^{p_k}, \Delta^{p_k-1} \rangle| / \|\Delta^{p_k}\|^2$ 
8        $x_{k+1} = \sum_{i=0}^{p_k} \binom{p_k}{i} (\sigma_k^{(p_k)})^i \Delta^i$ 
9   end for

```

Note: To improve global convergence, constraints on $\sigma_k^{(p_k)}$ may be imposed at step 7 and bounds checking on x_{k+1} at step 8. Also, a preliminary mapping before step 3 may improve the convergence of certain algorithms. See Section 4 for implementation detail.

Section 3 shows that for linear maps, Algorithm 1 produces a sequence x_k converging to a fixed point of F . Before presenting the proof, the advantage of alternating orders may be illustrated by revisiting the linear example of Barzilai and Borwein (1988) with $A = \text{diag}(20, 10, 2, 1)$, $b = (1, 1, 1, 1)^\top$, starting point $x_0 = (0, 0, 0, 0)^\top$ and solution $x^* = (20^{-1}, 10^{-1}, 2^{-1}, 1)^\top$. The convergence of ACX^{3,2} will be compared with that of ACX², a purely squared scheme equivalent to the CBB method in the linear case. The stopping criterion is $\|\Delta x_k\|_2 \leq 10^{-8}$. Figure 1 shows the trajectory of $|e_1|$ on the horizontal axis and $|e_2|$ on the vertical axis for both algorithms. The starting point is $(20^{-1}, 10^{-1})$ at the top right. The ACX² method needs 34 gradient evaluations before convergence but the ACX^{3,2} only needs 20 (meanwhile, the BB method requires 25 gradient evaluations and steepest descent needs 314). On the ACX² trajectory shown in dotted lines, each iteration accomplishes a mild reduction of the errors. Substantial decrease of $|e_2|$ only occurs at iteration 5. The ACX^{3,2} trajectory in dash-dotted lines shows errors being annihilated more aggressively; $|e_1|$ and $|e_2|$ must only be reduced substantially twice before convergence. While the benefits of alternating are not always so large for small linear examples, Section 5 will show how significant they can be in nonlinear multivariate contexts.

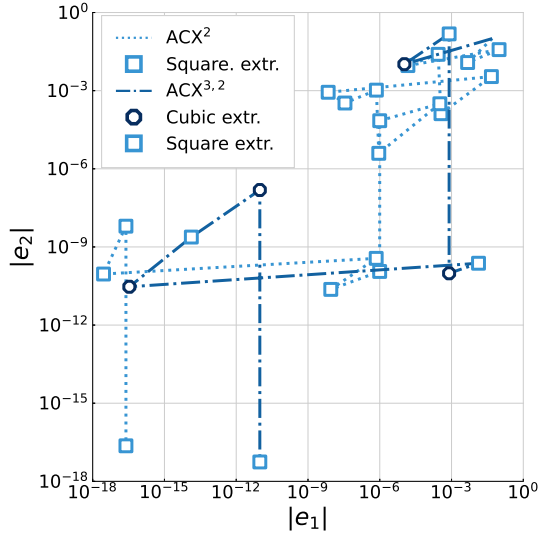


Figure 1: Convergence of $|e_1|$ and $|e_2|$ for the linear system, from initial values of $(1/20, 1/10)$ towards the solution $(0, 0)$ for ACX^2 and $ACX^{3,2}$

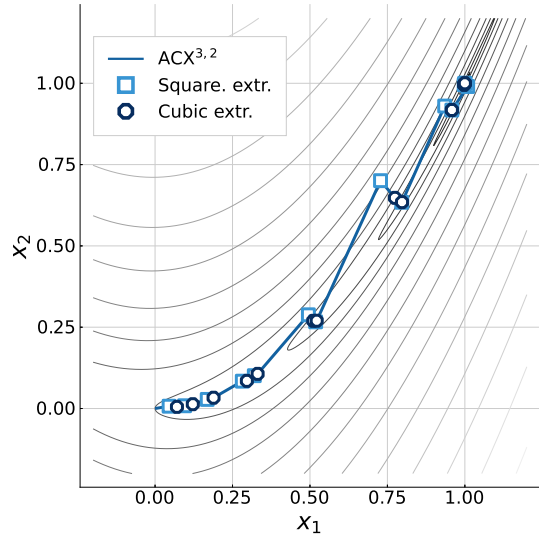


Figure 2: Convergence of $ACX^{3,2}$ for the 2-parameter Rosenbrock function from $(0,0)$ towards the solution $(1,1)$

3 Convergence of ACX

Studying the convergence of ACX systematically for linear systems of equations is a good approximation for the behavior of a general mapping F around its fixed point x^* . Raydan and Svaiter (2002) has shown that the CBB method converges Q-linearly in an appropriate norm. The following proof extends the result to any ACX algorithm.

Consider the linear system of equations defined $Qx = b$ where Q is symmetric positive definite. Define the elliptic norm

$$\|x\|_{Q^{-1}} = \sqrt{x^T Q^{-1} x}$$

induced by the inner product $\langle \cdot, \cdot \rangle_{Q^{-1}}$

$$\langle x, y \rangle_{Q^{-1}} = x^T Q^{-1} y.$$

The inner product satisfies the Cauchy-Schwarz inequality:

$$\|x\|_{Q^{-1}}^2 \cdot \|y\|_{Q^{-1}}^2 \geq \langle x, y \rangle_{Q^{-1}}^2$$

for vectors x, y .

To simplify the following computation, let us introduce the function

$$q_p(e) = e^T Q^p e.$$

for some vector e and the special case $q_p(e_k) \equiv q_p$ for e_k . Since Q is positive definite, $q_p(e) \geq 0 \forall p \in \mathbb{R}$. Observe notably that $\|e\|_{Q^{-1}}^2 = e^\top Q^{-1} e = q_{-1}(e)$.

Finally, let us introduce a useful lemma proven in appendix:

Lemma 1 For x, y , elements of a commutative ring, and $p \in \mathbb{N}^+ \setminus \{0, 1\}$, $(x + y)^p$ may be decomposed as

$$(x + y)^p = x^p + y^p - \sum_{i=1}^{\lfloor p/2 \rfloor} p(p-i-1)! \frac{(-xy)^i (x+y)^{p-2i}}{i! (p-2i)!}. \quad (8)$$

where $\lfloor a \rfloor$ outputs the greatest integer less than or equal to a .

Theorem 1 The sequence $\{x_k\}$ generated by the ACX^{p_1, \dots, p_P} method (7) applied to the mapping $F(x) = x - (Qx - b)$ converges Q -linearly in the norm Q^{-1} for any set of values p_1, \dots, p_P with $p_j \geq 2$.

Proof. After a p -order extrapolation, the error e_{k+1} may be expressed as

$$e_{k+1} = (I - \sigma_k^{(p)} Q)^p e_k,$$

where $p \geq 2$ is the extrapolation order at iteration k and $\sigma_k^{(p)} = \frac{|-e_k^\top Q^{2p-1} e_k|}{e_k^\top Q^{2p} e_k} = \frac{q_{2p-1}}{q_{2p}}$.

The squared Q^{-1} norm of e_{k+1} is

$$\|e_{k+1}\|_{Q^{-1}}^2 = \left\| (I - \sigma_k^{(p)} Q)^p e_k \right\|_{Q^{-1}}^2 = e_k^\top (I - \sigma_k^{(p)} Q)^p Q^{-1} (I - \sigma_k^{(p)} Q)^p e_k.$$

Rearrange the terms on the right hand side:

$$\|e_{k+1}\|_{Q^{-1}}^2 = e_k^\top Q^{-1} (I - \sigma_k^{(p)} Q) (I - \sigma_k^{(p)} Q)^{2p-1} e_k.$$

Rewrite the last parenthesis of the right hand side using (1) to get

$$\|e_{k+1}\|_{Q^{-1}}^2 = e_k^\top Q^{-1} (I - \sigma_k^{(p)} Q) \left[\sum_{i=1}^{\lfloor (2p-1)/2 \rfloor} c(p, i) (\sigma_k^{(p)} Q)^i (I - \sigma_k^{(p)} Q)^{2p-1-2i} \right] e_k.$$

where $c(p, i) = \frac{(2p-1)(2p-i-2)!}{i!(2p-1-2i)!}$. Note that $p \in \mathbb{N}^+ \setminus \{0, 1\} \rightarrow \lfloor (2p-1)/2 \rfloor = p-1$.

Multiplying back the terms outside the bracket and simplifying using the $q_p(e)$ notation, we get

$$q_{-1}(e_{k+1}) = q_{-1} - \sigma_k^{(p)} q_0 - (\sigma_k^{(p)})^{2p-1} (q_{2p-2} - \sigma_k^{(p)} q_{2p-1}) - \sum_{i=1}^{p-1} c(p, i) (\sigma_k^{(p)})^i q_{-1} (Q^{i/2} (I - \sigma_k^{(p)} Q)^{p-i} e_k).$$

where $q_{-1}(Q^{i/2} (I - \sigma_k^{(p)} Q)^{p-i} e_k) = e_k^\top (I - \sigma_k^{(p)} Q)^{p-i} Q^{i-1} (I - \sigma_k^{(p)} Q)^{p-i} e_k$. Factoring the first q_{-1} of the right hand side, rewrite the expression as

$$q_{-1}(e_{k+1}) = q_{-1} \cdot (1 - \theta_1 - \theta_2 - \theta_3)$$

where

- $\theta_1 = \sigma_k^{(p)} \frac{q_0}{q_{-1}}$
- $\theta_2 = \frac{(\sigma_k^{(p)})^{2p-1}}{q_{-1}} (q_{2p-2} - \sigma_k^{(p)} q_{2p-1}) = \frac{(\sigma_k^{(p)})^{2p-1}}{q_{-1} q_{2p}} (q_{2p-2} q_{2p} - q_{2p-1}^2)$
- $\theta_3 = \sum_{i=1}^{p-1} c(p, i) (\sigma_k^{(p)})^i \frac{q_{-1} (Q^{i/2} (I - \sigma_k^{(p)} Q)^{p-i} e_k)}{q_{-1}(e_k)}$.

Let us now show that $\theta_1 \geq \frac{\lambda_{\min}}{\lambda_{\max}}$, $\theta_2 \geq 0$, and $\theta_3 \geq 0$. Note that θ_1 may be written as the ratio of two Rayleigh quotients, with $\sigma_k^{(p)} = \frac{q_{2p-1}}{q_{2p}} = \left(\frac{q_{2p}}{q_{2p-1}} \right)^{-1} = \left(\frac{e_k^\top Q^{p-1/2} Q Q^{p-1/2} e_k}{e_k^\top Q^{p-1/2} Q^{p-1/2} e_k} \right)^{-1} \in [\lambda_{\max}^{-1}, \lambda_{\min}^{-1}]$ and $\frac{q_0}{q_{-1}} = \frac{e_k^\top Q^{-1/2} Q Q^{-1/2} e_k}{e_k^\top Q^{-1/2} Q^{-1/2} e_k} \in [\lambda_{\min}, \lambda_{\max}]$. Hence, $\theta_1 = \frac{q_{2p-1}}{q_{2p}} \frac{q_0}{q_{-1}} \in \left[\frac{\lambda_{\min}}{\lambda_{\max}}, \lambda_{\min} \right]$.

Further, note that

$$\begin{aligned} q_{2p-2} &= e_k^\top Q^{2p-2} e_k = \|Q^{p-1/2} e_k\|_{Q^{-1}}^2 \\ q_{2p} &= e_k^\top Q^{2p} e_k = \|Q^{p+1/2} e_k\|_{Q^{-1}}^2 \\ q_{2p-1} &= e_k^\top Q^{2p-1} e_k = \langle Q^{p+1/2} e_k, Q^{p-1/2} e_k \rangle_{Q^{-1}}. \end{aligned}$$

By the Cauchy-Schwarz inequality,

$$q_{2p-2} q_{2p} - q_{2p-1}^2 = \|Q^{p-1/2} e_k\|_{Q^{-1}}^2 \cdot \|Q^{p+1/2} e_k\|_{Q^{-1}}^2 - \langle Q^{p+1/2} e_k, Q^{p-1/2} e_k \rangle_{Q^{-1}}^2 \geq 0.$$

Hence,

$$\theta_2 = \frac{(\sigma_k^{(p)})^{2p-1}}{q_{-1} q_{2p}} (q_{2p-2} q_{2p} - q_{2p-1}^2) \geq 0.$$

Finally, for θ_3 , note that $c(p, i) > 0$ for $p \geq 2, i \leq p-1$ and that all $\frac{q_{-1} (Q^{i/2} (I - \sigma_k^{(p)} Q)^{p-i} e_k)}{q_{-1}(e_k)}$ terms are Rayleigh quotients with minimum of zero when $\sigma_k^{(p)} = \frac{1}{\lambda_r}$, $r \in \{1, \dots, n\}$.

Thus, we have

$$\frac{\|e_{k+1}\|_{Q^{-1}}}{\|e_k\|_{Q^{-1}}} = \sqrt{1 - \theta_1 - \theta_2 - \theta_3} \leq \sqrt{\frac{\lambda_{\max} - \lambda_{\min}}{\lambda_{\max}}}$$

which establishes the result. ■

We may convince ourselves that this linear convergence result is representative of any nonlinear mapping F in a neighborhood close to its fixed point x^* . Taking a first-order Taylor approximation of F applied p times:

$$F^p(x) = x^* + J^p \cdot (x - x^*) + o(x - x^*)$$

where J is the Jacobian of F at x^* . For a p -order difference, we have

$$\Delta^p x = (J - I)^p e + o(e).$$

Applying a p -order extrapolation from x_k (near x^*), the error at iteration $k + 1$ may be expressed as

$$e_{k+1} = (I - \sigma_k^{(p)}(I - J))^p e_k + o(e_k).$$

Hence, in a small neighborhood of x^* , ACX^{3,2} and ACX^{3,3,2} for nonlinear mappings should exhibit similar convergence as a linear map.

Theorem 1 also shows that from any starting point x_k in the neighborhood of x^* , all p -order extrapolation show the same worst case scenario of $\sqrt{1 - \lambda_{\min}/\lambda_{\max}}$. What differentiates ACX is its ability to make better scenarios more likely.

Away from x^* , $J(x)$ may change substantially between each mapping, and even more between extrapolations. Convergence is not guaranteed, but alternating between squared and cubic extrapolations may be advantageous like hybrid optimization algorithms are. Switching among constituent algorithms helps escape situations such as zigzagging or locally flat objective functions where a single algorithm would struggle. In fact, Roland and Varadhan (2004) did mention that SQUAREM – a purely squared extrapolation scheme – sometimes experiences near stagnation or breakdown when Δx and $\Delta^2 x$ are nearly orthogonal and s^{BB1} or s^{BB2} are used. For ACX^{3,2} and ACX^{3,3,2}, the probability that Δx and $\Delta^2 x$ be orthogonal and that $\Delta^2 x$ and $\Delta^3 x$ also be orthogonal is lower. The next section discusses implementation strategies to strike a good balance between speed and stability away from x^* .

4 Implementation detail and stability

This section discusses implementation detail of ACX in various situations. The proposed set of parameter values show good empirical properties but others could probably work well too.

Adaptive step size for gradient descent acceleration

Consider minimizing the function f by gradient descent. The mapping is

$$F(x) = x - \alpha \nabla f(x).$$

To be amenable to ACX acceleration, the descent step size α must be constant within each extrapolation cycle. It must also remain within an acceptable range of values since ACX is based on second- and third-order differences. An excessively small α may lead to small $\Delta^2 x$ or $\Delta^3 x$ and large $\sigma^{(2)}$ or $\sigma^{(3)}$, resulting in imprecise extrapolations when f has weak curvature. An excessively large α could on the other hand lead to zigzagging and at worst divergence of the algorithm.

A simple adaptive procedure for α can improve the chance $\sigma^{(p)}$ remains within reasonable bounds as often as possible. The initial step size is the largest possible α_0 which *i*) satisfies the Armijo–Goldstein condition (Armijo (1966)): $f(x_0 - \alpha_0 \nabla f(x_0)) \leq f(x_0) - c_{AG} \alpha_0 \|\nabla f(x_0)\|$ where $c_{AG} \in (0, 1)$ is some constant and *ii*) does not result in

a large increase in the gradient norm: $\|\nabla f(x_0 - \alpha_0 \nabla f(x_0))\|_2 \leq L_n \|\nabla f(x_0)\|_2$ where $L_n \geq 1$ is some constant.² After each iteration k , set $\alpha_{k+1} = \alpha_k \theta$ if $\sigma_k^{(p)} < \underline{L}_\sigma$ and $\alpha_{k+1} = \alpha_k / \theta$ if $\sigma_k^{(p)} > \bar{L}_\sigma$ where $\theta > 1$ and where \underline{L}_σ and $\bar{L}_\sigma > \underline{L}_\sigma$ are lower and upper thresholds within which $\sigma_k^{(p)}$ should preferably remain. The rationale for this simple step function is that $\sigma_k^{(p)}$ sometimes take very large or very small values for a single iteration. Overcorrecting α_{k+1} based on such iteration would be a disproportionate response and lead to worse results in the following iterations. In the empirical section, the parameters are set to $c_{AG} = 0.25$, $L_n = 2$, $\theta = 1.5$, $\underline{L}_\sigma = 1$ and $\bar{L}_\sigma = 2$.³

Accelerating mappings other than gradient descent

Constraining $\sigma^{(p)}$

For mappings with guaranteed improvement in the objective such as the EM algorithm, the step length may be constrained to $\underline{\sigma}^{(p)} = \max(1, \sigma^{(p)})$. Otherwise, in some scenarios, $|\langle \Delta^p x, \Delta^{p-1} x \rangle|$ could be close to zero, making $\sigma^{(p)}$ small as well and leading to slow progress. If the underlying mapping has guaranteed progress, then $\underline{\sigma}^{(p)} = 1$ ensures that ACX makes the same progress as the last mapping.⁴

Stabilization mappings

In many mapping applications such as the EM algorithm or the Majorize-Minimization (MM) algorithm (Lange (2016)), the mapping $F(x_k)$ takes the form of a constrained optimization given the parameter values of the previous iteration. For example, for the MM algorithm, the objective function $f(x)$ is maximized iteratively by the constrained maximization of a surrogate function $g(x)$. The mapping is $F(x_k) = \arg \max_x g(x|x_{k-1})$. Since the starting point x_0 is not in general a constrained maximum, the value of the objective function f can improve significantly following the first iteration. In the subsequent iterations, progress is typically much slower as x_k steadily converges from constrained maximum to constrained maximum toward its fixed point. This also means that the change in x after the first mapping may be sizable but be comparatively modest in the following iterations. Since ACX relies on extrapolation, using this initial mapping may provide little information on the true direction of the fixed point. To

²Additionally, to stabilize the start of ACX^{3,2} and ACX^{3,3,2}, $\sigma_0^{(2)}$ is computed at the first iteration. If it is below 1, a sign α is rather large, the algorithm starts with a squared extrapolation (an interpolation in that case) rather than a cubic one.

³Note that near the optimum, if α_k is small, $\Delta^p x_k$ may be too small for machine precision and lead to an imprecise $\sigma_k^{(p)}$. This is prevented with a progressive approach. Whenever $\|\Delta^p x_k\|_\infty$ is small considering the available machine precision ($\|\Delta^p x_k\|_\infty < 10^{-50}$ in the applications), $\sigma_k^{(p)}$ is set to 1 and α_{k+1} is set to $\min(1, 2^{1+t} \alpha_k)$, where t is the total number of times the same situation has occurred in the past.

⁴This was also suggested by Roland and Varadhan (2008). Note that it would not be appropriate for applications where we often have $\sigma^p \in (0, 1)$, such as the mapping operators considered by Lemaréchal (1971) with Lipschitz constants $L \in (0, 1)$. To limit zigzagging, a solution is replacing F by $F \circ F$.

improve the accuracy of the extrapolation, an initial “stabilization mapping” may be computed before each extrapolation. In practice, it is difficult to anticipate whether convergence will improve sufficiently to warrant the investment in this extra mapping. In the applications, it was beneficial for the Poisson mixture application, for ACX² specifically, and not beneficial for the other applications.

Non-monotonicity

ACX does not guarantee steady improvement in the objective at every iteration. Monotonicity could be enforced for ACX by either reducing the step size or simply falling back on a recent iterate with guaranteed improvement. This however may not be beneficial. Consider Figure 2 showing the convergence of ACX^{3,2} for the two-variable Rosenbrock function starting from (0, 0). As can be seen from the contour lines, some of the most fruitful steps toward the minimum (1, 1) are also causing temporary setbacks in the value of the objective. But the lost progress is quickly regained a few steps later. Ample testing has shown that reducing the size of these steps to enforce monotonicity often slows down convergence, sometimes dramatically. Since a fast algorithm is more valuable than a slow monotonic one, it was not implemented.

4.1 Backtracking

In rare occasions, the algorithm may reach parameter values where the gradient is undefined or infinite. Such outcome may be the result of $\sigma^{(p)}$ being too large or, for gradient descent, α being too large. In these situations, the following procedure is proposed.

The algorithm resumes at the best past iterate, labeled k_B , either the one with the smallest norm ($\|\nabla f(x_{k_B})\|$ or $\|\Delta x_{k_B}\|$), or with the smallest objective value $f(x_{k_B})$. To increase the stability of the extrapolation, replace $\sigma_{k_B+i}^{(p)} \rightarrow \rho_\sigma \sigma_{k_B+i}^{(p)}$ for $i = 1, 2, \dots$ with $0 < \rho_\sigma < 1$. For gradient descent acceleration, also replace $\alpha_{k_B+1} \rightarrow \rho_\alpha \alpha_{k_B+1}$ where $0 < \rho_\alpha < 1$, (and adjust α as usual in the following iterations). If the norm or the objective eventually improves, the algorithm resumes with normal extrapolation step lengths. If a new infeasible iterate occurs before an improvement, the algorithm backtracks again to k_B and restarts a second time with reductions $(\rho_\alpha^2, \rho_\sigma^2)$. Then, in case of failure, with $(\rho_\alpha^3, \rho_\sigma^3), \dots$. Such successive reductions in $\sigma^{(p)}$ and α should eventually lead to progress in a similar way to regular gradient descent with backtracking and make algorithm failure unlikely. In the empirical section, $\rho_\alpha = \rho_\sigma = 2$.

4.2 Bounds checking

Stalling may occur if an extrapolation leads to a saddle point or to a portion of the parameter space where $F(x)$ is defined but Δx is very small. Bound checks may prevent this situation. If such problematic parameter region is known to the users. Let $S \in \mathbb{R}^n$ be the set of feasible starting points that may be represented as the Cartesian product

of n open intervals: $S = \prod_{i=1}^n I^{(i)}$ where $I^{(i)} = (x_{\min}^{(i)}, x_{\max}^{(i)})$ $i \in (1, \dots, n)$. This simple representation – sometimes referred to as a box constraint – is appropriate in many applications but could potentially be generalized. Let $x_k \in S$ be a starting point and x_{k+1} be the next extrapolation. The next iterate with bounds checks is

$$\bar{x}_{k+1}^{(i)} = \max(\min(x_{k+1}^{(i)}, \omega x_{\max}^{(i)} + (1 - \omega)x_k^{(i)}), \omega x_{\min}^{(i)} + (1 - \omega)x_k^{(i)}) \quad i \in (1, \dots, n)$$

where $\omega \in (0, 1)$. This strategy keeps each $\bar{x}_{k+1}^{(i)}$ within bounds and ensures that no extrapolation covers more than a fraction ω of the distance between $x_{\max}^{(i)} - x_k^{(i)}$ or $x_k^{(i)} - x_{\min}^{(i)}$. A bound may still be reached asymptotically if it does contain the fixed point x^* . Note that the same bounds checking may be performed with gradient descent acceleration after each mapping to implement constrained optimization.

5 Applications

This section compares ACX to fast alternatives. For gradient descent acceleration, the minimization problems are a multivariate Rosenbrock function with or without constraints, a logistic regression, and 96 unconstrained problems from the CUTEst collection. For general mapping acceleration, the applications are the EM algorithm for a Poisson admixture model, the EM algorithm for a proportional hazard regression with interval censoring, alternating least squares (ALS) applied to rank tensor decomposition, the power method for finding dominant eigenvalues, and the method of alternating projection (von Neumann (1950), Halperin (1962)) applied to regressions with high-dimensional fixed effects.

Since the various algorithms vary greatly in terms of gradient and objective evaluations as well as internal computation, their performances are assessed by CPU time, presented via the performance profiles of Dolan and Moré (2002). These graphs show how often each algorithm was within a certain multiple of the best compute time. Appendix B also shows the average number objective function evaluations, gradient evaluations or mappings, evaluation time (for the draws that converged), and convergence rates.

Most computations were performed in Julia⁵ with the exception of the tensor canonical decomposition performed in MATLAB and the alternating projections application which compares packages of various languages. The benchmark stopping criterion was $\|\nabla f(x)\|_{\infty} \leq 10^{-7}$ for gradient descent acceleration and $\|\Delta x\|_{\infty} \leq 10^{-7}$ for general mapping applications. To ensure meaningful comparisons, draws for which different algorithms converged on divergent objective values were discarded. The precise condition was

$$|f(x_{T,i}) - \min_j(f(x_{T,j}))| < 10^{-5} \quad \forall i, \quad (9)$$

⁵Its just-in-time compiler guarantees little computing overhead. This is important to get accurate ideas of the relative number of operations required for each method.

where $x_{T,i}$ is the final iterate of any algorithm i , and $\min_j(f(x_{T,j}))$ is the minimum over all final iterates j , including for algorithms that have not converged. This rather stringent criterion was introduced with the CUTEst problems in mind. For each application, 2000 draws were computed, except for the CUTEst problems and the alternating projections application. In all applications, the gradient norm was used to track the progress of ACX. For each application, Appendix B presents additional implementation detail and statistics. Information on software, package versions and hardware used is provided in Appendix C.

Gradient descent applications

For gradient descent applications, the performances of ACX², ACX^{3,2} and ACX^{3,3,2} were compared with the L-BFGS algorithm and a N-CG method from the package Optim.jl (Mogensen and Riseth (2018)). The L-BFGS is implemented with Hager-Zhang line search and a window of 10 past iterates to build the Hessian approximation. The N-CG is also implemented with Hager-Zhang line search. The algorithm combines features of Hager and Zhang (2006) and Hager and Zhang (2013) and multiple revisions to the code since publication.

The Rosenbrock function

The Rosenbrock is a well-known test bed for new algorithms. The test specification involved finding the unconstrained minimum of a 1000-parameter version of the function

$$f(x^{(1)}, \dots, x^{(N)}) = \sum_{i=1}^{N/2} \left[100 \left((x^{(2i-1)})^2 - x^{(2i)} \right)^2 + (x^{(2i-1)} - 1)^2 \right] \quad N = 1000.$$

For the unconstrained minimization, the starting points $x_0^{(i)}$ were drawn from uniform distributions $U[-5, 5]$. A constrained minimization was also implemented with upper bound $x_{\max}^{(i)}$ sampled from $U[0, 1]$ and starting points $x_0^{(i)}$ sampled from $U[-5, 0]$. For L-BFGS and N-CG, the constraint was implemented with barrier penalty using Optim.jl's `fminbox`.⁶

The unconstrained minimization results are displayed in Figures 3 as well as Appendix Table 3. The three ACX algorithms show advantageous performances in terms of gradient evaluations, objective evaluations and compute time, with ACX^{3,3,2} being fastest 80% of the time.

The constrained minimization results are shown in Figure 4 and Appendix Table 4. Here, the simple box constraint implementation of Section 4.2 applied to gradient descent combined with ACX is surprisingly efficient. It is 30 to 40 times faster than

⁶See <https://juliansolvers.github.io/Optim.jl/stable/#user/minimization/#box-constrained-optimization> and <https://github.com/JuliaNLSolvers/Optim.jl/blob/adc5b277b3f915c25233b45f8f2dd61006815e63/src/m> for more detail.

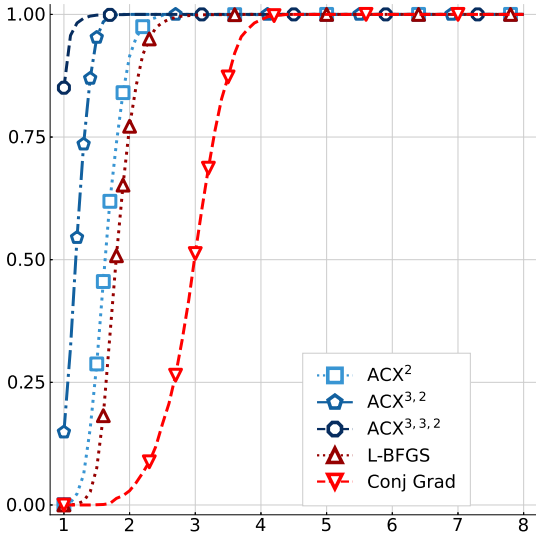


Figure 3: Performance profiles for the Unconstrained 1000-parameter Rosenbrock

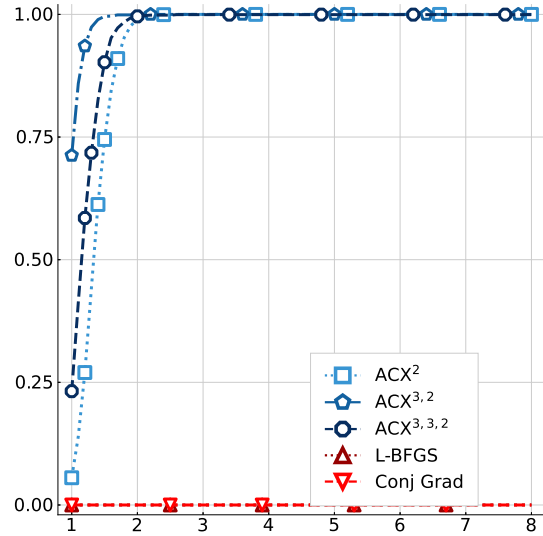


Figure 4: Performance profiles for the Constrained 1000-parameter Rosenbrock

L-BFGS or N-CG with barrier penalty. This encouraging result suggests ACX could also be efficient with a more general set of linear and non-linear constraints.

A logistic regression

An advantage of ACX is its limited reliance on objective functions. This may provide clear benefits for an application like the logistic regression for which the log likelihood requires taking logs:

$$l(y|X, \beta) = \sum_{i=1}^n [y_i \times x_i^T \beta - \log(1 + \exp(x_i^T \beta))],$$

where $y \in \mathbb{R}^n$, $X \in \mathbb{R}^{n \times m}$, but the gradient does not.

To illustrate this advantage, a simulation was conducted with $n = 2000$, $m = 100$, with coefficients and the covariates drawn from uniform distributions $U[-1, 1]$ and X containing a column of ones. For each draw, the starting point was $\beta_0 = \mathbf{0}$. The obvious speed gains from $ACX^{3,2}$ and $ACX^{3,3,2}$ can be seen in Figure 5. Appendix Table 5 shows $ACX^{3,2}$ and $ACX^{3,3,2}$ needed slightly fewer gradient evaluations than the alternatives and close to no objective function evaluations, making them 6 times faster than the L-BFGS and 10 times faster than the N-CG.

The set of unconstrained minimization problems from the CUTEst suite

The CUTEst problem set – successor of CUTE (Constrained and Unconstrained Testing Environment) and CUTER – has become the benchmark for prototyping new optimization algorithms. For testing, the unconstrained problems with objective function

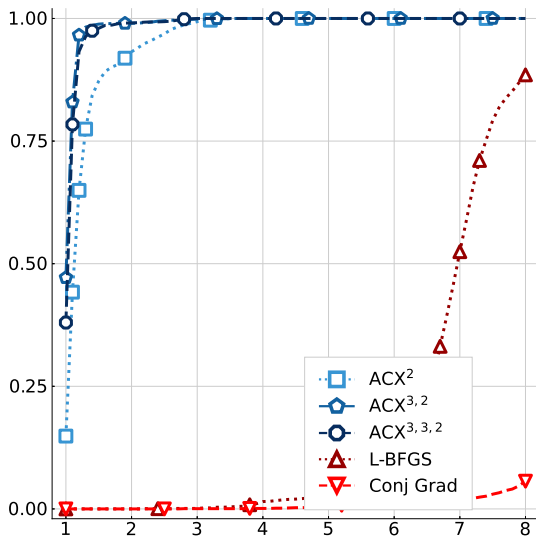


Figure 5: Performance profiles for the logistic regression

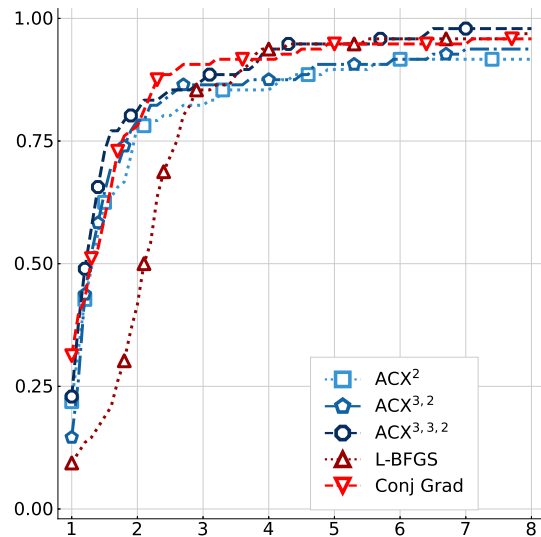


Figure 6: Performance profiles for 96 unconstrained optimization from the CUTEst collection (each problem is one draw)

defined as either quadratic, sum of squares or “other” were selected, numbering 154 in January 2021. Of these were excluded those with a zero initial gradient or with fewer than 50 parameters. When possible, the default number of parameters was used. When it was below 50, the number was set to 50 or 100 if available.

Algorithms were allowed to run for at most 100 seconds. A problem was excluded if no algorithm converged before 10 seconds or if all algorithms converged in fewer than 5 mappings. To avoid stalling, the initial stopping criterion was $\|\nabla f(x)\|_\infty < 10^{-5}$. When the final objectives diverged such that criterion (9) was not met, the tolerance was progressively decreased, down to $\|\nabla f(x)\|_\infty < 10^{-8}$. If the result still diverged, the number of parameters was reduced. In the end, 96 problems were kept for comparison.

The resulting performance profiles displayed in Figure 6 show $ACX^{3,3,2}$ outperforming the other ACX and frequently the other algorithms as well. The N-CG also did very well while the L-BFGS was often slower. The detail on the number of gradient and objective function evaluations, compute time, convergence status and minimum objective attained is available at sites.google.com/site/nicolaslepagesaucier/output_CUTEst.txt.

Various mapping applications

The EM algorithm for Poisson admixture model

The EM algorithm is a ubiquitous method in statisticians’ toolbox. While stable, it can be notoriously slow to converge, motivating the development of many acceleration methods.

A classic implementation of the EM algorithm is Hasselblad (1969) who models of

the death notices of women over 80 years old reported in the London Times over a period of three years. Table 1 reproduces the data.

Table 1: Number of death notices

Observed death count (i)	0	1	2	3	4	5	6	7	8	9
Frequency of occurrence (y_i)	162	267	271	185	111	61	27	8	3	1

The data are modeled as a mixture of two Poisson distributions to capture higher death rates during winter. The likelihood is

$$L(y^{(0)} \dots y^{(9)} | \mu^{(1)}, \mu^{(2)}, \pi) = \prod_{i=0}^9 \left[\pi e^{-\mu^{(1)}} \frac{(\mu^{(1)})^i}{i!} + (1 - \pi) e^{-\mu^{(2)}} \frac{(\mu^{(2)})^i}{i!} \right]^{y^{(i)}}$$

where μ_1 and μ_2 are the means of the distributions of subpopulations 1 and 2 and π is the probability that a random individual is part of subpopulation 1. The EM algorithm map is

$$\mu_{k+1}^{(1)} = \frac{\sum_{i=0}^9 y^{(i)} i w_k^{(i)}}{\sum_{i=0}^9 y^{(i)} w_k^{(i)}}, \mu_{k+1}^{(2)} = \frac{\sum_{i=0}^9 y^{(i)} i (1 - w_k^{(i)})}{\sum_{i=0}^9 y^{(i)} (1 - w_k^{(i)})}, \pi_{k+1} = \frac{\sum_{i=0}^9 y^{(i)} w_k^{(i)}}{\sum_{i=0}^9 y^{(i)}}$$

where

$$w_k^{(i)} = \frac{\pi_k e^{-\mu_k^{(1)}} (\mu_k^{(1)})^i}{\pi_k e^{-\mu_k^{(1)}} (\mu_k^{(1)})^i + (1 - \pi_k) e^{-\mu_k^{(2)}} (\mu_k^{(2)})^i}.$$

For the experiments, random starting points were sampled from uniform distributions $\pi_0 \sim U[0.05, 0.95]$, $\mu_0^{(i)} \sim U[0, 20]$ $i = 1, 2$. ACX was implemented with bound checks $\mu^{(i)} \geq 0$ $i = 1, 2$ and $\pi \in [0, 1]$ with a buffer of $\omega = 0.9$ and stabilization mapping. Its performances were compared with those of QNAMM (3) and DAAREM (2)⁷, both adapted to Julia from their respective R packages.

The results are displayed in Figure 7 and appendix Table 6. With only three parameters to estimate, ACX^{3,2} performed slightly better than ACX^{3,3,2}. Both outperformed QNAMM (3) and DAAREM (2) on all metrics, probably a result of the need to check the objective and their general computational burdens.

The EM algorithm for proportional hazard regression with interval censoring

Another common application of the EM algorithm is the mixed proportional hazard model. Wang et al. (2016) proposed a new method for estimating a semiparametric proportional hazard model with interval censoring, a common complication arising in medical and social studies. Their EM estimation relies on a two-stage data augmentation with latent Poisson random variables and a monotone spline representation of the

⁷As recommended by the authors, we use $\min(10, \lceil n/2 \rceil)$ lags where n is the number of parameters.

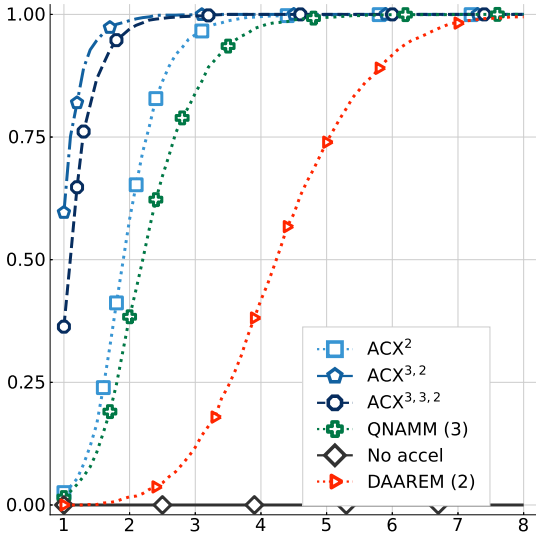


Figure 7: Performance profiles for the EM algorithm acceleration of Poisson admixtures

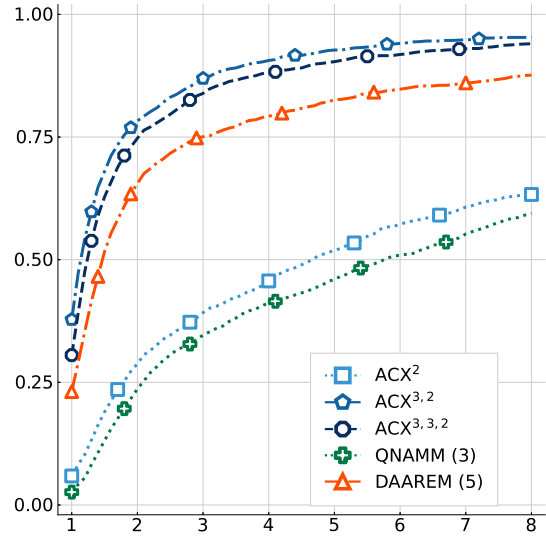


Figure 8: Performance profiles for the EM algorithm for proportional hazard regression with interval censoring

baseline hazard function. The algorithm is light and simple to implement (see Wang et al. (2016) for details) yet may benefit greatly from acceleration.

The simulation settings and codes of Henderson and Varadhan (2019) were adapted to Julia to allow for meaningful comparison. The likelihood for an individual observation is

$$L(\delta_1, \delta_2, \delta_3, \mathbf{x}) = F(R|\mathbf{x})^{\delta_1} \{F(R|\mathbf{x}) - F(L|\mathbf{x})^{\delta_2}\} \{1 - F(L|\mathbf{x})^{\delta_3}\}$$

where δ_1 , δ_2 , and δ_3 indicate either right-, interval-, and left-censoring, respectively. The failure time T is generated from the distribution $F(t, \mathbf{x}) = 1 - \exp\{-\Lambda_0(t) \exp(x^\top \beta)\}$ and the baseline risk is simulated as $\Lambda_0(t) = \log(1 + t) + t^{1/2}$. The covariates are $\mathbf{x} = \{x_1, x_2, x_3, x_4\}$ where $x_1, x_2 \sim N(0, 0.5^2)$ and $x_3, x_4 \sim \text{Bernoulli}(0.5)$. A censored interval is simulated by first generating $Y \sim \text{Exponential}(1)$ and setting either $(L, R) = (Y, \infty)$ if $Y \leq T$ or $(L, R) = (0, Y)$ if $Y > T$. The baseline risk is modeled as a six-parameter I-spline, for a total of 10 parameters to estimate. The sample size is set to 2000 individuals.

Since the algorithms always converged on widely different objective values, the allowed discrepancy was set to 2. The results are displayed in Figure 8 and appendix Table 7. $\text{ACX}^{3,2}$ was the top performer in terms of CPU time and mappings used, followed by $\text{ACX}^{3,3,2}$. Both outperformed DAAREM (2), ACX^2 and QNAMM (3). The non-accelerated EM algorithm took orders of magnitudes longer to converge.

Alternating least squares for tensor rank decomposition

ALS is an iterative method used in matrix completion, canonical tensor decomposition and matrix factorization used in online rating systems, signal processing, vision and

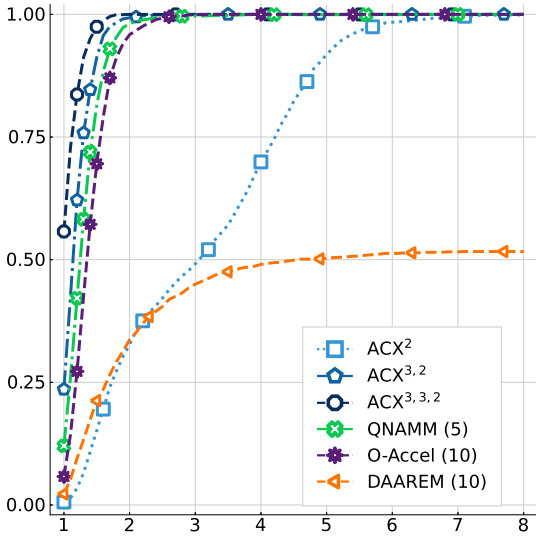


Figure 9: Performance profiles for the canonical vector decomposition

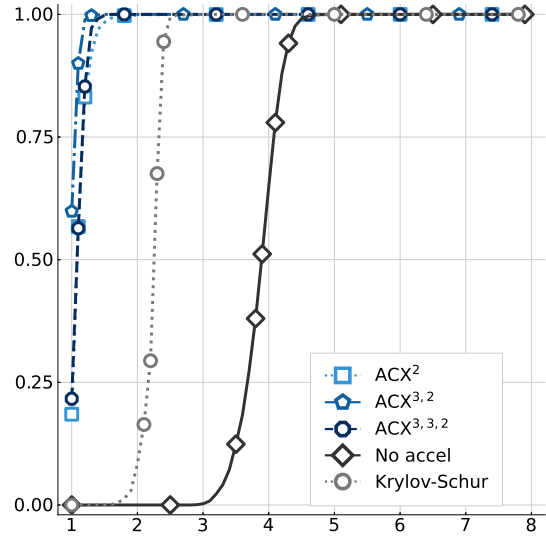


Figure 10: Performance profiles for the power method for dominant eigenvalues

graphics, psychometrics, and computational linguistics. For canonical tensor decomposition, De Sterck (2012) has designed an iterative algorithm combining an ALS step and the nonlinear generalized minimal residual method (N-GMRES) (Saad and Schultz (1986)). Riseth (2019) improved on the approach with a general-purpose acceleration method named objective acceleration (O-ACCEL).

The performance of O-ACCEL was compared to those of ACX and other general-purpose acceleration using De Sterck (2012)’s main test specification. First introduced by Tomasi and Bro (2006) and Acar et al. (2011), the test involves computing a 450-variable approximation of a three-way tensor of size $50 \times 50 \times 50$ with collinearity and noise (see the code for detail). For the tests, Riseth (2019)’s MATLAB code was adapted and ACX, QNAMM and DAAREM algorithms were written in MATLAB by the author. ACX was implemented with $\sigma = 1$. O-ACCEL and DAAREM worked best with a window of 10 past iterates and QNAMM worked well with a window of 5 past iterates. Less performant algorithms like the N-GMRES or L-BFGS were not tested.

The results are summarized in Figure 9 and appendix Table 8. $ACX^{3,3,2}$ had a clear but moderate advantage, closely followed by $ACX^{3,2}$ and QNAMM. O-ACCEL required fewer mappings on average but its heavier computational burden made it slightly slower.

The power method for dominant eigenvalues

Several big data applications with sparse structures involve computing a few dominant eigenvalues for which iterative approaches like the power method are clearly preferred. Given a diagonalizable matrix Q , the power method computes the eigenvector associated with the dominant eigenvalue of Q by combining matrix-vector multiplications

and rescaling:

The power method

Start with a non-zero vector x_0 .

Compute $x_{k+1} = \frac{Qx_k}{\|Qx_k\|_\infty}$ until convergence.

Under mild assumptions, the method generates a series of vectors x_k converging to an eigenvector associated with the largest eigenvalue of Q in magnitude. Unfortunately, the method may be slow to converge if the absolute value of ratio of the first and second largest eigenvalues is close to one. Jennings (1971) proposed accelerating it using the same multivariate version of Aitken’s Δ^2 process suggested by Lemaréchal (1971). In the same vein, we expect for good acceleration using ACX schemes.

For the test, a symmetric 1000×1000 sparse matrix was generated with 10% non-zero elements drawn from $U[0, 1]$. Random $U[0, 100]$ were added to the diagonal elements, creating a wide spectrum with similar magnitudes to the first and second eigenvalues.

ACX was compared with the unaccelerated power iteration and with the Krylov-Schur algorithm, implemented in KrylovKit.jl (see Saad (2000)). The results are displayed in Figures 10 and in Table 9. All ACX schemes performed well, taking around 3 milliseconds, while the Krylov-Schur took over 6 milliseconds and the unaccelerated power iteration took over 10 milliseconds.

Alternating projections for high-dimensional fixed-effects models

Following von Neumann (1949), finding the intersection between closed subspaces has been an active area of research in numerical methods (see Escalante and Raydan (2011) for a good treatment of the topic). The method of alternating projections is a simple algorithm for finding such intersection. Unfortunately, it can be arbitrarily slow to converge if the Friedrichs angle between the subspaces is small, spawning a large literature on faster algorithms. A noteworthy contribution was made by Gearhart and Koshy (1989) who suggested a generalized Aitken’s acceleration method (Scheme 3.4 in their paper). Since their method actually corresponds to Lemaréchal’s method applied to the cyclic projection algorithm (alternating projections applied sequentially to 2 or more subspaces), ACX constitutes a natural extension.

An interesting application to illustrate the potential of ACX and alternating projections is a method suggested by Gaure (2013). In social sciences and epidemiological studies, researchers often measure the impact of a few variables on large samples of potentially time-varying observations while controlling for stable unobserved effects. These could be worker effects, firm effects, school effects, teacher effects, doctor effects, hospital effects, etc. An example using public data is Head et al. (2010) who estimated the impact of colonial relations on trade flows. Rather than reproducing their exact results, consider the simple model

$$\ln x_{ijt} = c_{ijt}\beta + d_{it}\gamma_1 + d_{jt}\gamma_2 + d_{ij}\gamma_3 + u_{ijt} \tag{10}$$

where x_{ijt} is the export volume from country of origin i to country destination j in year t (keeping only non-zero trade flows). Colonial status is captured by c_{ijt} , a dummy variable that equals 1 if country i is still a colony of country j in year t , and u_{ijt} represents unobserved trade costs between the two countries at time t . The fixed effects are dummies capturing observed or unobserved factors affecting trade flows of the origin country at time t (d_{it}), of the destination country at time t (d_{jt}) and stable characteristics of the exporter-importer dyad such as common language, distance, etc. (d_{ij}). The parameter β should capture the impact of being a colony on log exports to the metropolitan state. Since colonial status is potentially correlated with the fixed effects, omitting them from the model would most likely bias the estimate of β .

The full sample of trading countries totals 707,368 observations and, more importantly, the model contains $9569 + 9569 + 29,603 = 48,741$ fixed effects. Needless to say, ordinary least squares estimation is impractical purely in terms of memory. In contrast, the method proposed by Gaure (2013) is fast and lightweight. Define x and c as column vectors containing the x_{ijt} and c_{ijt} , respectively, and $D = [D_{it}, D_{jt}, D_{ij}]$ as the matrix of fixed effects. The method employs the Frisch-Waugh-Lovell theorem (Frisch and Waugh (1933), Lovell (1963)) to estimate β by regressing $M_D x$ on $M_D c$, where $M_D = I - D(D^\top D)^{-1} D^\top$ projects onto the orthogonal complement of the column space of D . To avoid computing M_D directly, the method uses Halperin (1962)’s Theorem 1: $M_D = \lim_{k \rightarrow \infty} (M_{D_{it}} M_{D_{jt}} M_{D_{ij}})^k$. Since the projections onto each set of fixed effects are equivalent to simple group demeaning, the algorithm can be very fast and has become standard packages in many programming languages.

The potential pitfalls of alternating projections remain, however. If the panel is not well balanced and different sets of dummies are near collinear, convergence may require many iterations and take longer than alternative algorithms. In such cases, ACX acceleration could provide discernible benefits.

Gaure’s method was used to estimate (10), with and without ACX acceleration, with a stopping criterion of $\|\Delta x\|_2 \leq 10^{-8}$. For comparison, the same estimation was done with variety of equivalent packages in Julia, R, Python, and Stata. The R and Python packages implement Gaure’s method. In Julia, FixedEffectModel.jl uses the LSMR algorithm (Fong and Saunders (2011)) based on the Golub-Kahan bidiagonalization (Golub and Kahan (1964)). For reghdfe, see Correia (2016). To test for the impact of collinearity, the same model was estimated on the full sample and on a subsample excluding the 25% trading partners with the longest geographical distance, making trading blocs more localized and the panel less balanced.

Table 2 displays the CPU time and average mapping for the demeaning of x and c , performed independently. For the whole sample, ACX acceleration only provided a modest advantage over the unaccelerated alternating projections. For the partial sample however, the unaccelerated alternating projections was slower than LSMR, but ACX^{3,3,2} reduced the number of mappings and the compute time by 65% and was again the fastest overall.

Table 2: Performances for the trade flows regression with high-dimensional fixed effects

Algorithm / Package	Whole sample		Partial sample	
	Maps	Time (sec.)	Maps	Time (sec.)
No acceleration	21	0.41	82	0.80
ACX ²	16	0.31	26	0.32
ACX ^{3,2}	16.5	0.31	25	0.29
ACX ^{3,3,2}	16	0.29	24	0.28
FixedEffectModel (LSMR) (Julia)		0.52		0.42
FELM (R)		0.84		0.90
FixedEffectModel (Python)		2.75		5.84
reghdfe (Stata)		6.69		6.01
Observations		707,368		530,504

Notes: Maps display the average number of iterations to demean x and c . For Python, the time only includes demeaning. Python and R both use Gaure (2013)’s method as well, but do not display the number of mappings. Stata’s reghdfe is too different for a meaningful comparison of the number of mappings.

6 Discussion

This article has introduced new acceleration methods for fixed-point iterations. By alternating between squared and cubic extrapolations, the ACX schemes target specific error components and dynamically speed-up convergence in subsequent iterations. Thanks to cycling, the extra computation needed for cubic extrapolations is essentially free. For linear systems, ACX is Q-linear convergent.

Many optimization methods and fixed-point iteration accelerations store information from past iterates, making them efficient in some contexts but possibly less so in others. By only extrapolating from two or three mappings, ACX schemes are remarkably fast, stable, and versatile. Applied to gradient descent, they are competitive with the best nonlinear solvers. They also speed up other fixed-point iterations like the EM algorithm, ALS, the power method, and the method of alternating projections. These represent a small subset of potential uses, which may extend to image processing, physics, and other big data applications with sparse representations.

References

- Acar, E., Dunlavy, D. and Kolda, T. (2011). A scalable optimization approach for fitting canonical tensor decompositions. *Journal of Chemometrics* 25: 67–86.
- Armijo, L. (1966). Minimization of functions having Lipschitz continuous first partial derivatives. *Pacific Journal of Mathematics* 16: 1–3.

- Barzilai, J. and Borwein, J. (1988). Two-point step size gradient methods. *IMA Journal of Numerical Analysis* 8: 141–148.
- Bezanson, J., Edelman, A., Karpinski, S. and Shah, V. B. (2017). Julia: A fresh approach to numerical computing. *SIAM review* 59: 65–98.
- Birgin, E., Martínez, J. and Raydan, M. (2014). Spectral projected gradient methods: Review and perspectives. *Journal of Statistical Software* 60: 1–21.
- Bongartz, I., Conn, A. R., Gould, N. and Toint, P. L. (1995). CUTE: Constrained and unconstrained testing environment. *ACM Trans. Math. Softw.* 21: 123–160, doi: 10.1145/200979.201043.
- Brezinski, C. and Chehab, J. (1998). Nonlinear hybrid procedures and fixed point iterations. *Numerical Functional Analysis and Optimization* 19: 465–487.
- Brezinski, C. and Redivo-Zaglia, M. (2020). *Extrapolation and Rational Approximation*. Springer Nature Switzerland.
- Brezinski, C., Redivo-Zaglia, M. and Saad, Y. (2018). Shanks sequence transformations and Anderson acceleration. *SIAM Review* 60: 646–669.
- Correia, S. (2016). Linear models with high-dimensional fixed effects: An efficient and feasible estimator. Tech. rep., Duke University, working paper.
- Dai, Y.-H., Huang, Y. and Liu, X.-W. (2019). A family of spectral gradient methods for optimization. *Computational Optimization and Applications* 63: 43–65.
- De Sterck, H. (2012). A nonlinear GMRES optimization algorithm for canonical tensor decomposition. *SIAM Journal on Scientific Computing* 34: A1351–A1379.
- Dempster, A., Laird, N. and Rubin, D. (1977). Maximum likelihood from incomplete data via the EM algorithm. *Journal of the Royal Statistical Society: Series B (Methodological)* 39: 1–38.
- Dolan, E. and Moré, J. (2002). Benchmarking optimization software with performance profiles. *Mathematical Programming* 91: 201–213.
- Escalante, R. and Raydan, M. (2011). *Alternating Projection Methods*. SIAM. Society for Industrial and Applied Mathematics.
- Fong, D. and Saunders, M. (2011). LSMR: An iterative algorithm for sparse least-squares problems. *SIAM Journal on Scientific Computing* 33: 2950–2971.
- Friedlander, A., Martínez, J., Molina, B. and Raydan, M. (1999). Gradient method with retards and generalizations. *SIAM Journal on Numerical Analysis* 36: 275–289.

- Frisch, R. and Waugh, F. (1933). Partial time regressions as compared with individual trends. *Econometrica* 1: 387–401.
- Gaure, S. (2013). OLS with multiple high dimensional category variables. *Computational Statistics and Data Analysis* 66: 8–18.
- Gearhart, W. and Koshy, M. (1989). Acceleration schemes for the method of alternating projections. *Journal of Computational and Applied Mathematics* 26: 235–249.
- Golub, G. and Kahan, W. (1964). Calculating the singular values and pseudo-inverse of a matrix. *Journal of the Society for Industrial and Applied Mathematics Series B Numerical Analysis* 2: 205–224.
- Hager, W. and Zhang, H. (2006). Algorithm 851: CG DESCENT, a conjugate gradient method with guaranteed descent. *ACM Transactions on Mathematical Software* 32: 113–137.
- Hager, W. and Zhang, H. (2013). The limited memory conjugate gradient method. *SIAM Journal on Optimization* 23: 2150–2168.
- Halperin, I. (1962). The product of projection operators. *Acta Scientiarum Mathematicarum (Szeged)* 23: 96–99.
- Hasselblad, V. (1969). Estimation of finite mixtures of distributions from the exponential family. *Journal of the American Statistical Association* 64: 1459–1471.
- Head, K., Mayer, T. and Ries, J. (2010). The erosion of colonial trade linkages after independence. *Journal of International Economics* 81: 1–14.
- Henderson, N. and Varadhan, R. (2019). Damped Anderson acceleration with restarts and monotonicity control for accelerating EM and EM-like algorithms. *Journal of Computational and Graphical Statistics* 28: 834–846.
- Henrici, P. (1964). *Elements of numerical analysis*. R.E. Krieger Pub. Co.
- Irons, B. and Tuck, R. (1969). A version of the Aitken accelerator for computer iteration. *International Journal of Numerical Methods in Engineering* 1: 275–277.
- Jbilou, K. and Sadok, H. (2000). Vector extrapolation methods. Applications and numerical comparison. *Journal of Computational and Applied Mathematics* 122: 149–165.
- Jennings, A. (1971). Accelerating the convergence of matrix iterative processes. *IMA Journal of Applied Mathematics* 8: 99–110.
- Lange, K. (2016). *MM Optimization Algorithms*. SIAM.

- Lebedev, V. and Zabelin, V. (1995). Combined trinomial iterative methods with Chebyshev parameters. *East-West Journal of Numerical Mathematics* 3: 145–162.
- Lemaréchal, C. (1971). Une méthode de résolution de certains systèmes non linéaires bien posés. In *Comptes rendus hebdomadaires des séances de l'Académie des sciences*, A, Sciences Mathématiques 272. Paris, France: Académie des sciences, 605–607.
- Liu, D. and Nocedal, J. (1989). On the limited memory BFGS method for large scale optimization. *Numerical optimization* 45: 497–528.
- Lovell, M. (1963). Seasonal adjustment of economic time series and multiple regression analysis. *Journal of the American Statistical Association* 58: 993–1010.
- Macleod, A. (1986). Acceleration of vector sequences by multi-dimensional Δ^2 methods. *Communications in Applied Numerical Methods* 2: 385–392.
- Marder, B. and Weitzner, H. (1970). A bifurcation problem in E-layer equilibria. *Plasma Physics* 12: 435–445.
- Mogensen, P. K. and Riseth, A. N. (2018). Optim: A mathematical optimization package for Julia. *Journal of Open Source Software* 3: 615, doi:10.21105/joss.00615.
- Nocedal, J. and Wright, S. (2006). *Numerical Optimization, Second Edition*. Springer Series in Operational Research. Springer, 2nd ed.
- Ortega, J. and Rheinboldt, W. (1970). *Iterative Solutions of Nonlinear Equations in Several Variables*. SIAM.
- Ramière, I. and Helfer, T. (2015). Iterative residual-based vector methods to accelerate fixed point iterations. *Computers and Mathematics with Applications* 70: 2210–2226.
- Raydan, M. and Svaiter, B. (2002). Relaxed steepest descent and Cauchy-Barzilai-Borwein method. *Computational Optimization and Applications* 21: 155–167.
- Riseth, A. (2019). Objective acceleration for unconstrained optimization. *Numerical Linear Algebra With Applications* 26: 1–17.
- Roland, C. and Varadhan, R. (2004). Squared Extrapolation Methods (SQUAREM): A New Class of Simple and Efficient Numerical Schemes for Accelerating the Convergence of the EM Algorithm. Working papers, Johns Hopkins University, Dept. of Biostatistics.
- Roland, C. and Varadhan, R. (2005). New iterative schemes for nonlinear fixed point problems, with applications to problems with bifurcations and incomplete-data problems. *Applied Numerical Mathematics* 55: 215–226.

- Roland, C. and Varadhan, R. (2008). Simple and globally convergent methods for accelerating the convergence of any EM algorithm. *Scandinavian Journal of Statistics* 35: 335–353.
- Saad, Y. (2000). *Iterative Methods for Sparse Linear Systems*. Society for Industrial and Applied Mathematics, 2nd ed.
- Saad, Y. and Schultz, M. (1986). GMRES: A generalized minimal residual algorithm for solving nonsymmetric linear systems. *SIAM Journal on Scientific Computing* 7: 856–869.
- Tomasi, G. and Bro, R. (2006). A comparison of algorithms for fitting the PARAFAC model. *Computational Statistics & Data Analysis* 50: 1700–1734.
- von Neumann, J. (1949). On rings of operators. Reduction theory. *Annals of Mathematics Second Series* 50: 401–485.
- von Neumann, J. (1950). *Functional Operators*. Princeton University Press.
- Wang, L., McMahan, C., Hudgens, M. and Qureshi, Z. (2016). A flexible, computationally efficient method for fitting the proportional hazards model to interval-censored data. *Biometrics* 72: 222–231.
- Zhou, H., Alexander, D. and Lange, K. (2011). A quasi-Newton acceleration for high-dimensional optimization algorithms. *Statistics and computing* 21: 261–273.

Appendix

A Proofs

Proof of Lemma 1. From the binomial formula, express $(x + y)^p$ as the sum of $x^p + y^p$ and an extra term:

$$\begin{aligned}
 (x + y)^p &= \sum_{j=0}^p \frac{p!}{j!(p-j)!} x^{p-j} y^j \\
 &= x^p + y^p + \sum_{j=1}^{p-1} \frac{p!}{j!(p-j)!} x^{p-j} y^j \\
 &= x^p + y^p + \sum_{j=0}^{p-2} \frac{p!}{(j+1)!(p-j-1)!} x^{p-j-1} y^{j+1} \\
 &= x^p + y^p + pxy(R_1)
 \end{aligned} \tag{11a}$$

where

$$R_1 = \sum_{j=0}^{p-2} \frac{p-1}{(j+1)(p-1-j)} \frac{(p-2)!}{j!(p-2-j)!} x^{p-2-j} y^j.$$

Consider the case of a general extra term:

$$R_i = \sum_{j=0}^{p-2i} \frac{i(p-i)}{(j+i)((p-i)-j)} \frac{(p-2i)!}{j!(p-2i-j)!} x^{p-2i-j} y^j.$$

Let us consider different cases. By direct calculation, if p is even and $i = p/2$, $R_i = 1$. If p is odd and $i = (p-1)/2$, $R_i = x + y$. If $1 \leq i < \lfloor p/2 \rfloor$, using the binomial formula:

$$R_i = (x+y)^{p-2i} + \sum_{j=0}^{p-2i} \left(\frac{i(p-i)}{(j+i)((p-i)-j)} - 1 \right) \frac{(p-2i)!}{j!(p-2i-j)!} x^{p-2i-j} y^j$$

$$R_i = (x+y)^{p-2i} - \sum_{j=0}^{p-2i} \frac{j}{j+i} \frac{p-2i-j}{p-i-j} \frac{(p-2i)!}{j!(p-2i-j)!} x^{p-2i-j} y^j.$$

If $j = 0$ or $j = p-2i$ then $\frac{j}{j+i} \frac{p-2i-j}{p-i-j} = 0$. We may therefore write

$$R_i = (x+y)^{p-2i} - \sum_{j=1}^{p-2i-1} \frac{j}{j+i} \frac{p-2i-j}{p-i-j} \frac{(p-2i)!}{j!(p-2i-j)!} x^{p-2i-j} y^j$$

and rewrite the sum as

$$R_i = (x+y)^{p-2i} - \sum_{j=0}^{p-2i-2} \frac{j+1}{j+1+i} \frac{p-2i-j-1}{p-i-j-1} \frac{(p-2i)!}{(j+1)!(p-2i-j-1)!} x^{p-2i-j-1} y^{j+1}$$

$$R_i = (x+y)^{p-2i} - \left[\sum_{j=0}^{p-2(i+1)} \frac{xy \frac{(p-2i)(p-2i-1)}{(i+1)(p-(i+1))} \times}{(j+i+1)(p-(i+1)-j)} \frac{(p-2(i+1))!}{j!(p-2(i+1)-j)!} x^{p-2(i+1)-j} y^j \right]$$

$$R_i = (x+y)^{p-2i} - xy \frac{(p-2i)(p-2i-1)}{(i+1)(p-i-1)} R_{i+1}.$$

By recursively substituting R_{i+1} back in 11a, we may rewrite the whole expression using a summation for $i = 1$ to $\lfloor p/2 \rfloor$ and recover (8). ■

B Tables of numerical results

Table 3: Average performances: Unconstrained Rosenbrock

Algorithm	Grad. evals	Obj. evals	Time (ms)	Conv.	Minimum
ACX ²	907.9	11.0	14.23	1.00	2.00E-15
ACX ^{3,2}	720.7	11.0	10.37	1.00	2.00E-15
ACX ^{3,3,2}	596.7	11.0	8.83	1.00	1.00E-15
L-BFGS	759.1	759.1	15.75	1.00	1.20E-14
N-CG	929.7	1855.4	25.56	1.00	3.00E-15

Note: 1000 parameters.

Table 4: Average performances: Constrained Rosenbrock

Algorithm	Grad. evals	Obj. evals	Time (ms)	Conv.	Minimum
ACX ²	458.0	6.0	9.18	1.00	1.98E+02
ACX ^{3,2}	358.6	6.0	7.08	1.00	1.98E+02
ACX ^{3,3,2}	408.2	6.0	8.14	1.00	1.98E+02
L-BFGS	4815.0	4815.0	295.95	1.00	1.98E+02
N-CG	3574.1	5006.7	266.78	1.00	1.98E+02

Notes: 1000 parameters. For ACX, $\omega = 0.999$.

Table 5: Average performances: Logistic regression

Algorithm	Grad. evals	Obj. evals	Time (sec.)	Conv.	Minimum
ACX ²	53.2	5.3	29.85	1.00	612.1403
ACX ^{3,2}	51.8	5.3	25.14	1.00	612.1403
ACX ^{3,3,2}	51.8	5.3	25.55	1.00	612.1403
L-BFGS	64.8	64.8	164.48	1.00	612.1403
N-CG	61.8	94.2	257.92	1.00	612.1403

Note: 100 parameters.

Table 6: Average performances: EM algorithm for Poisson admixture

Algorithm	Maps	Obj. evals	Time (ms)	Conv.	Minimum
ACX ²	102.1	0.0	0.53	1.00	1989.9459
ACX ^{3,2}	56.0	0.0	0.31	1.00	1989.9459
ACX ^{3,3,2}	61.1	0.0	0.33	1.00	1989.9459
QNAMM (3)	113.0	108.0	0.62	1.00	1989.9459
No acceleration	2524.0	0.0	11.35	1.00	1989.9459
DAAREM (2)	67.5	84.6	1.15	1.00	1989.9459

Notes: 3 parameters, 0.95% of draws rejected for discrepant results. ACX implemented with stabilization mapping and $\omega = 0.8$.

Table 7: Average performances: proportional hazards regression with interval censoring

Algorithm	Maps	Obj. evals	Time (sec.)	Conv.	Minimum
ACX ²	2562.1	0	4.84	0.885	952.5416754
ACX ^{3,2}	333.3	0	0.64	0.991	952.3066159
ACX ^{3,3,2}	394.3	0	0.74	0.993	952.2839194
QNAMM (3)	1840.3	1223.6	3.43	0.995	952.0988158
DAAREM (5)	752.2	1211.1	1.62	0.985	952.3447906

Notes: 10 parameters, 17.55% of draws rejected for discrepant results.

Table 8: Average performances: canonical tensor decomposition

Algorithm	Maps	Obj evals	Time (sec.)	Conv.	Minimum
ACX ²	228.3	57.4	1.74	1.00	0.0741
ACX ^{3,2}	90.0	18.4	0.68	1.00	0.0741
ACX ^{3,3,2}	82.9	15.9	0.62	1.00	0.0741
QNAMM (5)	88.8	81.8	0.74	1.00	0.0741
O-Accel (10)	56.6	56.6	0.8	1.00	0.0741
DAAREM (10)	556.5	606.5	1.15	0.52	0.0741

Notes: 450 parameters, 6.9% of draws rejected for discrepant results. One ALS iteration is registered as one mapping.

Table 9: Average performances: dominant eigenvalues

Algorithm	Maps	Time (ms)	Conv.
ACX ²	29.9	3.07	1.00
ACX ^{3,2}	28.0	2.83	1.00
ACX ^{3,3,2}	30.1	3.03	1.00
No acceleration	110.4	10.64	1.00
Krylov-Schur	53.7	6.14	1.00

Note: 1000 parameters.

C Software and hardware used

For the CUTEst and the alternating projections applications, each problem was run five times if the median time was over 0.1 seconds, and 100 times if it was below 0.1 seconds. Then the median time is reported. All tests in Julia were run once before recording time to exclude compile time. See the code for detail.

The main software used for the numerical experiments were Julia v.1.6.1 (Bezanson et al. (2017)), FixedEffectModels.jl v1.6.1, Optim.jl v1.3.0 (Mogensen and Riseth (2018)), CUTEst.jl v0.11.1, KrylovKit 0.5.3, MATLAB R2018a, Stata 13, reghdfe (Stata package), Python v3.8.5, FixedEffectModel v0.0.2 (Python), R v4.0.4, and felm (lfe v 2.8-6, R).

All computations were single-threaded, done on HP ZBooks 15 with Intel Core i7-4900MQ CPUs with 2.80GHz and 32 Go of RAM. All were done on Ubuntu 20.04, except the alternating projections using MATLAB on Windows 10.